International Journal of Multidisciplinary Innovative Research
ISSN: 2583-0228 Volume 6, Number 2 (April' 2026) pp. 98-105
© CIIR, Noida, INDIA (www.ciir.in)
https://www.ijmir.org

Received: 03 Jan' 2026 | Revised: 23 Mar' 2026 | Accepted: 28 Mar' 2026 | Published: 30 Mar' 2026

Original Article

OPEN ACCESS

An Experimental Investigation of Sol-Gel Derived Undoped and Rare-Earth Yttrium Doped ZnO Thin Films Along with Their Transistors

Bhawna[1], Anuj Kumar[2], Rashmi Singh[3], Karan Upadhaya[4], Dongjin Lee[5] and Manoj Kumar[6*]

[1,3]*Department of Physics, School of Physical Sciences, Starex University, Gurugram, India.*
[2]*Department of Physics, J. C. Bose University of Science & Technology, YMCA, Faridabad, India.*
[4,6]*Department of Physics, Harcourt Butler Technical University (HBTU), Kanpur, India.*
[5]*Department of Mechanical Engineering, Konkuk University, Gwangjin, Seoul, South Korea.*

Email: manoj.k@hbtu.ac.in[*]

Abstract: *In this report, the development of solution-processed sol-gel derived un-doped and rare-earth yttrium (Y) doped ZnO (Y-ZnO) thin films is presented. Both undoped and Y-ZnO thin films exhibited a highly preferred (002) c-axis orientation peak. The Y-ZnO thin film crystallinity was considerably improved with an increase of (002) peak intensity and grain size. O_{1s} spectra of X-ray photoelectron spectroscopy (XPS) showed less number of oxygen vacancy-related defects present in the Y-ZnO as compared to undoped ZnO. The fabricated thin film transistor (TFT) based on un-doped ZnO exhibited an on/off current ratio of 10^2 and field effect mobility of 0.0052 $cm^2\ V^{-1}\ s^{-1}$ and large threshold voltage respectively. However, Y-ZnO-based TFT showed an on/off current ratio exceeding 10^2, and electron mobility was achieved at 0.011 $cm^2\ V^{-1}\ s^{-1}$.*

Keywords: *ZnO Thin Films, Sol-Gel Method, Yttrium Doping, Thin Film Transistor (TFT), X-ray Diffraction (XRD), Electron Mobility, Rare-Earth Doping.*

INTRODUCTION

Due to a surge of interest in the development of thin film transistors (TFTs) for display device applications, ZnO has been intensively researched in the recent past. ZnO is one of the groups II-VI n-type compound semiconductors without any intentional doping with a wide bandgap of 3.37 eV at room temperature and a large exciton binding energy of 60 meV. Owing to its natural n-type conduction, ZnO has a large number of native defects such as oxygen vacancies. ZnO can be doped with group III elements to increase semiconductors' electron mobility and can reach values of 200 $cm^2V^{-1}s^{-1}$ at low doping levels [1-7]. A considerable amount of research is focused on indium gallium zinc oxide (InGaZnO) for fabricating TFTs and producing high-quality results which may be good enough for use in display devices [8, 9]. However, both In and Ga are expensive and rare elements on the earth making it unbearable to maintain the sustainability of large-scale production. Therefore, new materials need to be explored to

substitute these elements. Furthermore, ZnO-based display devices such as TFTs can easily form oxygen vacancies and generate excess free electrons. To control excess carriers, it is essential to dope suitable elements with lower electronegativity than that of Zn.

Moreover, Yttrium is an environmentally friendly and abundant rare earth element, and yttrium oxide (Y_2O_3) has several important properties such as a large band gap (~5.5 eV), high dielectric, and low electron negativity (1.22). The electrical properties of the active ZnO thin film layer can be easily controlled and modulated by doping Y in the ZnO thin films. In the recent past, several deposition techniques such as sol-gel, spray pyrolysis, sputtering, chemical vapor deposition, and molecular beam epitaxy have been widely used to grow ZnO.

An earlier study revealed that sol-gel and RF magnetron sputtering techniques are suitable techniques for fabricating Y-doped ZnO thin films. However, the sol-gel method has the advantage of coating large areas with easy control of doping and homogeneity compared to sputtering. Moreover, the sol-gel method is widely used for commercial production and even low-temperature deposited films are high quality stable, dense, and uniform.

In the present study, rare earth element Y is selected to dope ZnO to address this issue because Y has lower electronegativity as compared to Zn, which is expected to form stable ionic bonds between Y and O in the ZnO matrix. Therefore, it could be considered as a favorable semiconductor channel for display devices such as TFTs. ZnO-based TFTs are also developed and characterized by simple methods through solution-processed sol-gel derived methods.

EXPERIMENTAL DETAILS

A precursor solution of ZnO was prepared from zinc acetate ($Zn(CH_3CO_2)_2 \cdot 2H_2O$, purity 99.5%) dissolved in 2-methoxyethanol to obtain a solution concentration of 0.2 M. Then, Yttrium nitrate hexahydrate ($Y_2NO_3 \cdot 6H_2O$) was added to this solution as a dopant with varying concentration from 0.5% to 3%. Then, the as-prepared precursors were stirred for 2 h at room temperature to ensure that they were fully dissolved. The resultant solution was very clear, transparent, and homogenous and was used after 24 hrs for film deposition. The SiO_2 deposited Si substrates were cleaned using acetone and methanol for 10 min each and rinsed with DI water for 5 min. The prepared precursor solutions were then spin-coated at 4500 rpm for 30 s and the deposited films were dried on a hot plate at 150 °C for 10 min to eradicate possible solvents. This process was repeated several times to obtain the desired thickness of the deposited films. The thickness of un-doped and ZnO: Y thin film was around 70 nm.

For fabricated TFTs, SiO_2 deposited Si wafer substrate was chosen where Si served as the gate electrode, and 300-nm-thick thermally grown SiO_2 was used as the dielectric layer. In the last part, Al electrodes were fabricated by using thermal deposition method onto the semiconducting layer with the help of a shadow mask. The channel width and length were kept at 1500 and 150 µm, respectively. The source and drain electrode thickness was measured at about 120 nm.

Riggaku (Japan, D/max-II with Cu-K_α radiation) X-ray diffraction (XRD) was employed to study the crystallographic orientations of the films. The surface morphologies of the undoped ZnO and ZnO:Y thin films were examined using field-emission scanning electron microscopy (FE-SEM, S-4200 Hitachi, Japan). The optical transmittance measurements were carried out in the wavelength range of 200–800 nm using a double-beam SHIMADZU-330 spectrophotometer. Current-voltage (I–V) measurements were performed by using a semiconductor analyzer (Keithley 4200) with a probe station.

RESULTS AND DISCUSSION

Figure 1 shows XRD patterns of sol-gel derived un-doped ZnO and 2% doped Y-ZnO thin films. Both undoped ZnO and Y-ZnO thin films show (002), (102) and (103) diffraction peaks and (002) diffraction peaks exhibited the highest peak intensity, which indicates that the films have a preferred c-axis orientation. The (002) diffraction peak position of un-doped ZnO and Y-ZnO thin films are found to be at 34.06° and 34.22°, respectively. The lower 2θ value of the (002) peak position of the undoped ZnO thin film suggests the film is suffering from stress. However, In the case of Y-ZnO thin film, the peak position is shifted to a higher 2θ value from 34.06° to 34.22°, indicating reliving of stress in the films. There is a drastic increase of peak intensity along with reduced FWHM of (002) peak from 1.42 to 1.27°. It is assumed that Y^{3+} atoms replace the Zn^{2+} site with the Zn sites in the films and the surplus Y impurities tend to be positioned at interstitial position. This may be because of insufficient activation energy of impurity atoms. The crystallite size 't' was determined by using the Scherrer formula $t = \frac{0.9 \times \lambda}{B \cos \theta_B}$ [10]. Where λ is the x-ray wavelength (1.54060 Å), θ_B is the Bragg diffraction angle and B is the FWHM of (002) diffraction peak, respectively.

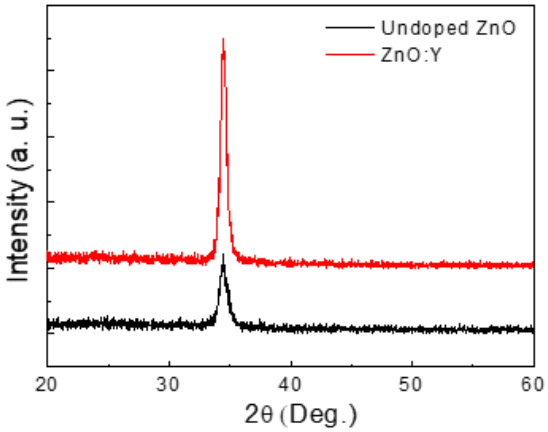

Figure 1: X-ray diffraction pattern of undoped ZnO and Y-ZnO thin films.

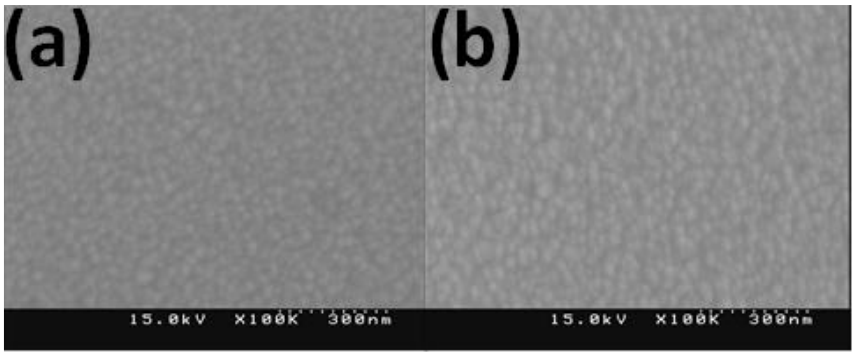

Figure 2: SEM images of (a) undoped ZnO and (b) Y-ZnO thin films.

The crystallite size of the films was examined to be 6.8 and 7.56 nm, respectively. The SEM micrograph of undoped ZnO and Y-ZnO thin films is shown in Figure 2 (a & b). The surface morphology of the film revealed a homogeneous surface formed with conforms-like grains. The Y-ZnO thin film showed slightly increased grain size in comparison to the ZnO thin film. The grain size determined from SEM micrographs 3.86 and 5.81 nm is consistent with the particle size calculated from the XRD result.

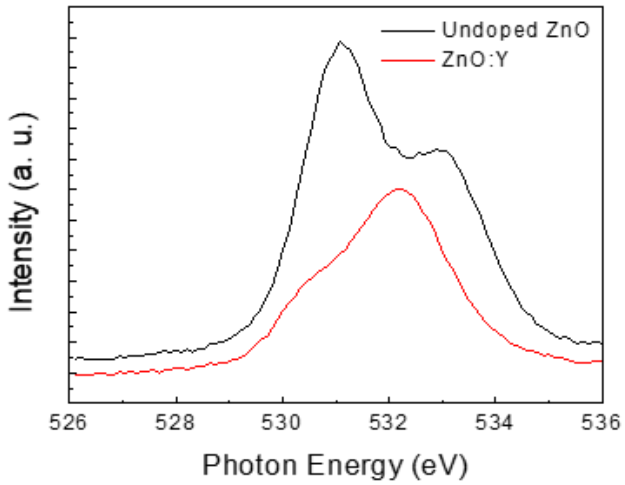

Figure 3: XPS spectra of undoped ZnO and Y-ZnO thin films.

Figure 3 shows the O_{1s} peak in the XPS spectrum of undoped ZnO and 2 at % doped Y-ZnO thin films. The O_{1s} spectra of undoped ZnO thin films exhibited a wide spectrum along with the peaks centered at 530.66, and 532.33 eV, respectively. However, the Y-ZnO thin films O_{1s} spectrum shows peaks at 530.8, 531.57, and 532.51 eV, respectively. The peak observed at 531.57 can be assigned to oxygen vacancies. The peak located at lower energy near 530.66-530.8 eV can be attributed to the O^{2-} ion at the intrinsic site (Zn-O bond) in the ZnO wurtzite structure. The peak at 532.33-532.51 eV centered at a higher energy side could be assigned to the existence of loosely bound oxygen on the surface of the ZnO thin film containing a certain species such as adsorbed O_2, $-CO_3$ and H_2O [11]. The loosely bound oxygen on the surface of the ZnO thin film containing to a certain species such as adsorbed O_2, $-CO_3$, and H_2O peak intensity is drastically reduced in Y-ZnO thin films. Mostly, the mobility of ZnO is affected by the association between oxygen lattice and oxygen vacancies. The existence of oxygen vacancies related peak and highly reduced oxygen bound on the surface of the ZnO in the Y-ZnO thin film indicates the relative quantity of oxygen-related defects increases. This may allow for enhancing mobility.

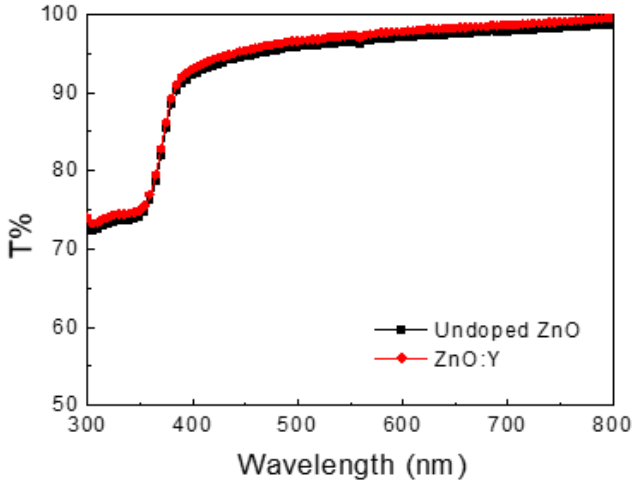

Figure 4: Transmission spectra of undoped ZnO and Y-ZnO thin films.

The obtained thin films exhibited very high optical transmittance. The optical transmittance of undoped and 2 at % doped Y-ZnO thin films was found to be around 96% as is depicted in Figure 4. The optical band gap of the ZnO films can be calculated from the relationship between

the optical absorption coefficient and the transmittance. The absorption coefficient α near the absorption edge is given by $\alpha = -\ln(T/d)$.

In the case of a direct band gap semiconductor, the optical band gap can be expressed by the Tauc model and parabolic bands $(\alpha h\nu)^2 = A(h\nu - Eg)$ [12]. Where A is a proportional constant, hν h is the photon energy of the incident light, and E_g is the optical band gap. The optical band gap is obtained by extrapolating the tangential line to the photon energy axis in the plot of $(\alpha h\nu)^2$ versus hν, as shown in Figure 5. The optical band gap for undoped ZnO and Y-ZnO thin films is estimated to be 3.24 and 3.26 eV.

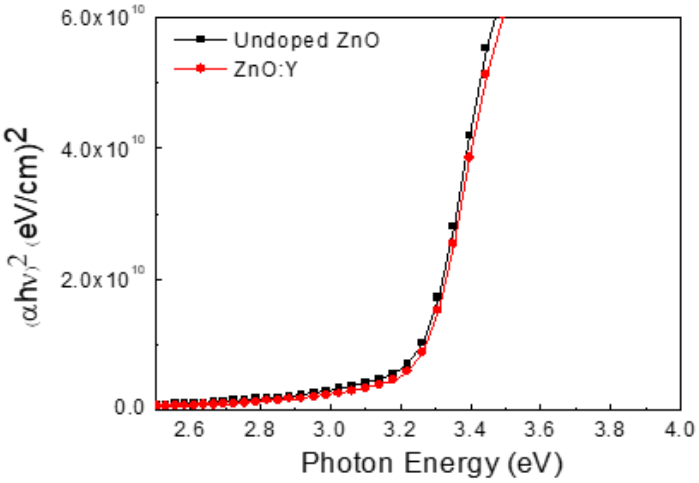

Figure 5: Plot of $(\alpha h\nu)^2$ versus hν of undoped ZnO and Y-ZnO thin films.

Earlier reported studies exhibited that the performance of the ZnO thin films can be improved by doping an appropriate amount of rare earth elements. In this study, Y element is selected for enhancement of the ZnO film properties, and it was observed that the density of Y elements occupying substitutional sites in the ZnO is found to be relatively low and surplus of Y dopant impurities incline to be sitting at interstitial positions.

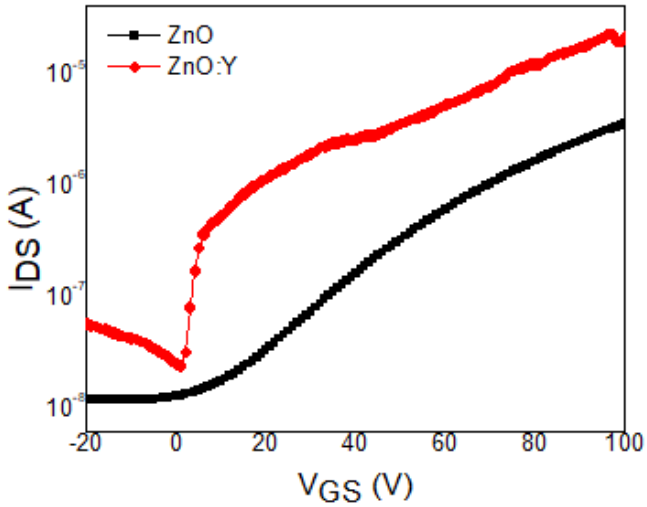

Figure 6: Transfer characteristics of undoped and Y-ZnO TFTs.

The transfer characteristics (I_{DS} vs V_{GS}) of the undoped ZnO and 2% doped Y-ZnO TFTs fabricated by sol-gel drive are presented in Figure 6. A clear enhancement accumulation mode transistor type characteristics of undoped ZnO and Y-ZnO TFTs were observed at low V_{DS} of 10 V. Low I_{on}/I_{off} ratio of the order of 10^2 was observed in the case of undoped ZnO TFTs.

However, the Y-ZnO TFTs showed enhanced operating characteristics and the I_{on}/I_{off} ratio significantly increased from the order of 10^2 to the high value of 10^4. The transistor parameters can be determined from the linear fit of the $(I_{Ds})^{1/2}$ vs. V_{GS} plot. The field effect mobility, and threshold voltage values of undoped ZnO TFT are examined to be 0.0052 cm^2/Vs, and 20.86 V, respectively. However, the mobility of Y-ZnO TFT is found to be higher and the obtained value is as high as 0.011 cm^2/Vs. The threshold voltage was reduced and observed to be -10.4 V, respectively. The mobility of ZnO is strongly dependent on the carrier concentration generated by oxygen vacancy formation. The significantly increased mobility and decreased sub-threshold voltage are attributed to extra oxygen vacancy formation in Y-ZnO. Conduction in the Y-ZnO channel layer is improved by Y doping in the ZnO. It is observed that the electrical results of undoped ZnO are lower because the formation of defects like oxygen or zinc vacancies does not get sufficient activation energy.

However, the results obtained suggest that the Y-ZnO TFT exhibited improved performance, which may be due to excess Y dopants occupying interstitial positions in the ZnO to create vacancies. These vacancies may act as scattering sites for electron mobility. Moreover, Y may substitute at oxygen in the ZnO and generate free electrons, which act as charge carriers thus enhancing the mobility of the Y-ZnO TFT. Further, the presence of hydroxyl groups produces an adverse effect on the TFTs' performance and these hydroxyl groups are highly suppressed in the Y-ZnO-based TFT, resulting in the enhancement of Y-ZnO TFT performance [13].

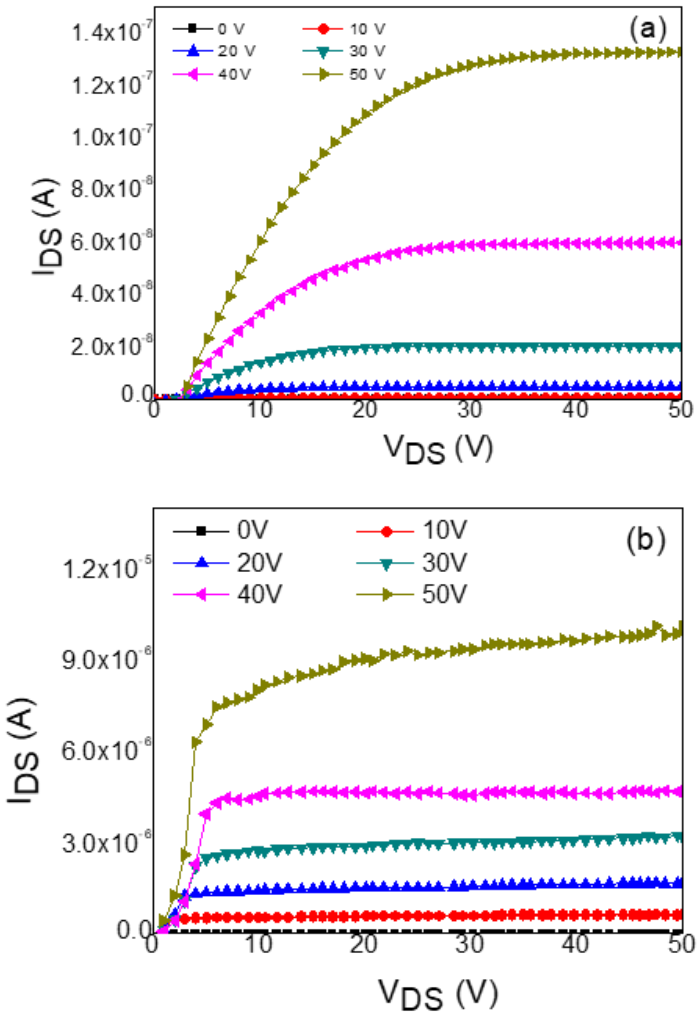

Figure 7: Output characteristics of (a) undoped ZnO and (b) Y-ZnO TFTs.

The output characteristics (I_{DS} vs. V_{DS}) of undoped ZnO and 2 at % doped Y-ZnO TFTs are depicted in Figure 6 (a) and (b). The gate-to-source voltage (V_{DS}) was varied from 0 to 50 V with a step increment of 10 V. The result obtained clearly revealed the typical behavior of TFT with an n-type active channel semiconductor layer. Pinch-off and current saturation are observed at various voltages (0–40 V), suggesting that the TFTs operated according to the standard field-effect transistor theory.

The main difference is observed in the saturation current level, which is increased by more than one order of magnitude in the case of Y-ZnO TFT. Further, the undoped ZnO output characteristics showed a large leakage current from the I_{DS} offset from zero with varying V_G from 0 to 40 V. On the other hand, Y-ZnO TFT output characteristics indicated no leakage current as the I_{DS} aligned at zero volts with varying V_G from 0 to 40 V.

CONCLUSION

Undoped ZnO and Y-ZnO thin films fabricated by solution processed sol-gel derived are demonstrated. It is important to note that XRD peak position corresponding to (002) diffraction peak of ZnO thin film is found to be close to bulk value, indicating forming minimum stress and peak position was slightly shifted from bulk value in the case of Y-ZnO thin film. The Y-ZnO thin film crystallinity was significantly enhanced with uniform and large grain size. The O_{1s} spectra of X-ray photoelectron spectroscopy (XPS) confirmed less number of oxygen vacancy related defects present in the Y-ZnO thin films as compare to undoped ZnO. Undoped ZnO and Y-ZnO TFTs are also developed. The obtained results showed considerable enhancement in the electrical properties of Y-ZnO TFTs in comparison to undoped ZnO TFT. The obtained results suggest that Y doping can be a useful approach to producing reliable and oxide–semiconductor-based TFTs derived from a sol-gel solution process.

ACKNOWLEDGMENT

The authors would like to thank Dr. Hakyung Jeong for his valuable suggestions in developing TFTs.

REFERENCES

[1] S. J. Kim, A. R. Song, S. S. Lee, S. Nahm, Y. Choi, K. B. Chung, and S. Jeong, *J. Mat. Chem. C*, vol. 3, pp. 1457, 2015.

[2] M. Esro, G. Vourlias, C. Somerton, W. I. Milne, and G. Adamopoulos, *Adv. Funct. Mater.*, vol. 25, pp. 134, 2015.

[3] H. W. Lee, M. Kim, J. H. Jun, U. Choi, and B. H. Lee, "Improving the performance of ultrathin ZnO TFTs using high pressure hydrogen annealing," *Nanomaterials*, vol. 15, no. 9, pp. 1484, 2025.

[4] J. Chang, Z. Lin, M. Lin, C. Zhu, J. Zhang, and J. Wu, *J. Mater. Chem. C*, vol. 3, pp. 1787, 2015.

[5] H. C. Liu, Y. C. Lai, C. C. Lai, B. S. Wu, H. W. Zan, P. Yu, Y. L. Chueh, and C. C. Tsai, *ACS Appl. Mater. Interfaces*, vol. 7, pp. 232, 2015.

[6] C. Avis, H. R. Hwang, and J. Jang, *ACS Appl. Mater. Interfaces*, vol. 6, pp. 10941, 2014.

[7] F. Liu, A. Sneck, P. Ekelinen, O. Helonen, L. Gillan, and J. Leppaniemi, "ALD-Grown ZnO TFTs Patterned by High-Resolution Reverse-Offset Printing," *ACS Appl. Mater. Interfaces*, vol. 17, pp. 34150–34160, 2025.

[8] P. T. Liu, Y. T. Chou, L. F. Teng, F. H. Li, and H. P. Shieh, *Appl. Phys. Lett.*, vol. 98, pp. 052102, 2016.

[9] A. Abliz, J. Wang, L. Xu, D. Wan, L. Liao, C. Ye, C. Liu, C. Jiang, H. Chen, and T. Guo, *Appl. Phys. Lett.*, vol. 108, pp. 213501, 2016.

[10] S. Cho, J. Ma, Y. Kim, Y. Sun, G. K. L. Wong, and J. B. Ketterson, *Appl. Phys. Lett.*, vol. 75, pp. 2761, 1999.

[11] G. H. Kim, H. S. Shin, B. D. Ahn, K. H. Kim, W. J. Park, and H. J. Kim, *J. Electrochem. Soc.*, vol. 156, no. 1, pp. H7, 2009.

[12] A. E. J. Gonzalez, J. A. S. Urueta, and R. J. S. Perra, *J. Cryst. Growth*, vol. 192, pp. 430, 1998.

[13] M. Kumar, H. Jeong, and D. Lee, *Superlattices & Microstructures*, vol. 120, pp. 395-401, 2018.